A New Parareal Algorithm for Time-Periodic Problems with Discontinuous Inputs

Martin J. Gander, Iryna Kulchytska-Ruchka, and Sebastian Schöps

1 Introduction

Time-periodic problems appear naturally in engineering applications. For instance, the time-periodic steady-state behavior of an electromagnetic device is often the main interest in electrical engineering, because devices are operated most of their life-time in this state. Depending on the size and complexity of the underlying system, the search for a time-periodic solution might however be prohibitively expensive. Special techniques were developed for the efficient computation of such solutions, like the *time-periodic explicit error correction method* [9], which accelerates calculations by correcting the solution after each half period, or the method presented in [1], which leads to faster computations of periodic solutions by determining suitable initial conditions.

The Parareal algorithm was invented in [10] for the parallelization of evolution problems in the time direction. A detailed convergence analysis when applied to linear ordinary and partial differential equations with smooth right-hand sides can be found in [6], for nonlinear problems, see [3]. In [5], a new Parareal algorithm was introduced and analyzed for problems with discontinuous sources. The main idea of the method is to use a smooth approximation of the original signal as the input for the coarse propagator. In [4], a Parareal algorithm for nonlinear time-periodic problems was presented and analyzed. Our interest here is in time-periodic steady-state solutions of problems with quickly-switching discontinuous excitation, for which we will introduce and study a new periodic Parareal algorithm.

Martin J. Gander
Section de Mathématiques, University of Geneva, 2-4 Rue du Lièvre, CH-1211 Geneva, Switzerland, e-mail: martin.gander@unige.ch

Iryna Kulchytska-Ruchka and Sebastian Schöps
Institut für Teilchenbeschleunigung und Elektromagnetische Felder, Technische Universität Darmstadt, Schlossgartenstrasse 8, D-64289 Darmstadt, Germany, e-mail: kulchytska@gsc.tu-darmstadt.de and e-mail: schoeps@temf.tu-darmstadt.de

2 Parareal for time-periodic problems with discontinuous inputs

We consider a time-periodic problem given by a system of ordinary differential equations (ODEs) of the form

$$\boldsymbol{u}'(t) = \boldsymbol{f}(t, \boldsymbol{u}(t)), \quad t \in \mathcal{I}, \qquad \boldsymbol{u}(0) = \boldsymbol{u}(T), \tag{1}$$

with the right-hand side (RHS) $\boldsymbol{f} : \mathcal{I} \times \mathbb{R}^n \to \mathbb{R}^n$ and $\boldsymbol{f}(0, \boldsymbol{v}) = \boldsymbol{f}(T, \boldsymbol{v})$ for all n-dimensional vectors $\boldsymbol{v}$ and the solution $\boldsymbol{u} : \mathcal{I} \to \mathbb{R}^n$ on the time interval $\mathcal{I} := (0, T)$.

In power engineering, electrical devices are often excited with a pulse-width-modulated (PWM) signal [2], which is a discontinuous function with quickly-switching dynamics. For applications such as motors or transformers a couple of tens of kHz might be used as the switching frequency [11]. To solve time-periodic problems of the form (1) supplied with such inputs with our new periodic Parareal algorithm, we assume that the RHS can be split into a sufficiently smooth bounded function $\bar{\boldsymbol{f}}$ and the corresponding discontinuous remainder $\tilde{\boldsymbol{f}}$ as

$$\boldsymbol{f}(t, \boldsymbol{u}(t)) := \bar{\boldsymbol{f}}(t, \boldsymbol{u}(t)) + \tilde{\boldsymbol{f}}(t), \quad t \in \mathcal{I}. \tag{2}$$

Such a decomposition can be achieved by a Fourier series expansion of the time-dependent input, then $\bar{\boldsymbol{f}}$ may be excited by a few principal harmonics, see [5].

We decompose $[0, T]$ into N subintervals $[T_{n-1}, T_n]$, $n = 1, \ldots, N$ with $T_0 = 0$ and $T_N = T$, and introduce the fine propagator $\mathcal{F}\big(T_n, T_{n-1}, \mathbf{U}_{n-1}^{(k)}\big)$ which computes an accurate solution at time T_n of the initial-value problem (IVP)

$$\boldsymbol{u}_n'(t) = \boldsymbol{f}(t, \boldsymbol{u}_n(t)), \quad t \in (T_{n-1}, T_n], \qquad \boldsymbol{u}_n(T_{n-1}) = \boldsymbol{U}_{n-1}^{(k)}. \tag{3}$$

The corresponding coarse propagator $\bar{\mathcal{G}}\big(T_n, T_{n-1}, \mathbf{U}_{n-1}^{(k)}\big)$ computes an inexpensive approximation at time T_n of the corresponding IVP having the reduced RHS $\bar{\boldsymbol{f}}(t, \boldsymbol{u}(t))$,

$$\bar{\boldsymbol{u}}_n'(t) = \bar{\boldsymbol{f}}(t, \bar{\boldsymbol{u}}_n(t)), \quad t \in (T_{n-1}, T_n], \qquad \bar{\boldsymbol{u}}_n(T_{n-1}) = \boldsymbol{U}_{n-1}^{(k)}. \tag{4}$$

Our new periodic Parareal algorithm then computes for $k = 0, 1, \ldots$ and $n = 1, \ldots, N$

$$\mathbf{U}_0^{(k+1)} = \mathbf{U}_N^{(k)}, \tag{5}$$

$$\mathbf{U}_n^{(k+1)} = \mathcal{F}\big(T_n, T_{n-1}, \mathbf{U}_{n-1}^{(k)}\big) + \bar{\mathcal{G}}\big(T_n, T_{n-1}, \mathbf{U}_{n-1}^{(k+1)}\big) - \bar{\mathcal{G}}\big(T_n, T_{n-1}, \mathbf{U}_{n-1}^{(k)}\big), \tag{6}$$

until the jumps at the synchronization points T_n, $n = 1, \ldots, N-1$ as well as the periodicity error between $\mathbf{U}_0^{(k)}$ and $\mathbf{U}_N^{(k)}$ are reduced to a given tolerance. The initial guesses $\mathbf{U}_n^{(0)}$, $n = 0, \ldots, N$ for (5)-(6) can be computed by

$$\boldsymbol{U}_n^{(0)} := \bar{\mathcal{G}}\big(T_n, T_{n-1}, \boldsymbol{U}_{n-1}^{(0)}\big), \quad n = 1, \ldots, N. \tag{7}$$

We note that the correction (5) does not impose a strict periodicity, but a relaxed one, since the end value at the kth iteration $\mathbf{U}_N^{(k)}$ is used to update the initial approximation $\mathbf{U}_0^{(k+1)}$ at the next iteration. This approach was introduced for time-periodic problems in [4] and was named PP-IC (which stands for *periodic Parareal with initial-value coarse problem*). In contrast to this method, where both coarse and fine propagators solve the IVP (3), our iteration (5)-(6) uses a reduced dynamics on the coarse level, described by (4). Convergence of the PP-IC algorithm was analysed in [4]. We extend this analysis now to the new Parareal iteration (5)-(6), applied to a model problem.

3 Convergence of the new periodic Parareal iteration

We consider the linear time-periodic scalar ODE

$$u'(t) + \kappa u(t) = f(t), \quad t \in (0,T), \qquad u(0) = u(T), \tag{8}$$

with a T-periodic discontinuous RHS $f : [0,T] \to \mathbb{R}$, a constant $\kappa \in \mathbb{R} : \kappa > 0$, and the solution function $u : [0,T] \to \mathbb{R}$ we want to compute.

In order to investigate the convergence of the new periodic Parareal algorithm (5)-(6) applied to (8), we introduce several assumptions. Let the time interval $[0,T]$ be decomposed into subintervals of equal length $\Delta T = T/N$. We assume that the fine propagator $\mathcal{F}$ is exact, and we can thus write the solution of the IVP for the ODE in (8) at T_n, starting from the initial value $U_{n-1}^{(k)}$ at T_{n-1} as

$$\mathcal{F}\left(T_n, T_{n-1}, U_{n-1}^{(k)}\right) = e^{-\kappa \Delta T} U_{n-1}^{(k)} + \int_{T_{n-1}}^{T_n} e^{-\kappa (T_n - s)} f(s) ds. \tag{9}$$

Next, introducing a smooth and slowly-varying RHS $\bar{f}$ by $f = \bar{f} + \tilde{f}$, we let the coarse propagator $\bar{\mathcal{G}}$ be a one-step method, applied to

$$\bar{u}_n'(t) + \kappa \bar{u}_n(t) = \bar{f}(t), \quad t \in (T_{n-1}, T_n], \qquad \bar{u}_n(T_{n-1}) = U_{n-1}^{(k)}. \tag{10}$$

Using the stability function $\mathcal{R}(\kappa \Delta T)$ of the one-step method, one can then write

$$\bar{\mathcal{G}}\left(T_n, T_{n-1}, U_{n-1}^{(k)}\right) = \mathcal{R}(\kappa \Delta T)\, U_{n-1}^{(k)} + \xi_n\left(\bar{f}, \kappa \Delta T\right), \tag{11}$$

where function ξ_n corresponds to the RHS discretized on $[T_n, T_{n-1}]$ with the one-step method. We also assume that

$$|\mathcal{R}(\kappa \Delta T)| + \left| e^{-\kappa \Delta T} - \mathcal{R}(\kappa \Delta T) \right| < 1. \tag{12}$$

Using (9) and (11) and following [4], the errors $e_n^{(k+1)} := u(T_n) - U_n^{(k+1)}$ of the new periodic Parareal algorithm (5)-(6) applied to the model problem (8) satisfy for

$n = 1, 2, \ldots, N$ the relation

$$\begin{aligned} e_n^{(k+1)} &= u(T_n) - \mathcal{F}\big(T_n, T_{n-1}, U_{n-1}^{(k)}\big) - \bar{\mathcal{G}}\big(T_n, T_{n-1}, U_{n-1}^{(k+1)}\big) + \bar{\mathcal{G}}\big(T_n, T_{n-1}, U_{n-1}^{(k)}\big) \\ &= e^{-\kappa\Delta T}\, u(T_{n-1}) + \int_{T_{n-1}}^{T_n} e^{-\kappa(T_n - s)} f(s) ds - e^{-\kappa\Delta T}\, U_{n-1}^{(k)} - \int_{T_{n-1}}^{T_n} e^{-\kappa(T_n - s)} f(s) ds \\ &\quad - \Big(\mathcal{R}\left(\kappa\Delta T\right) U_{n-1}^{(k+1)} + \xi_n\left(\bar{f}, \kappa\Delta T\right)\Big) + \Big(\mathcal{R}\left(\kappa\Delta T\right) U_{n-1}^{(k)} + \xi_n\left(\bar{f}, \kappa\Delta T\right)\Big) \\ &= \mathcal{R}\left(\kappa\Delta T\right) e_{n-1}^{(k+1)} + \Big(e^{-\kappa\Delta T} - \mathcal{R}\left(\kappa\Delta T\right)\Big) e_{n-1}^{(k)}. \end{aligned} \tag{13}$$

Similarly, the initial error satisfies $e_0^{(k+1)} = e_N^{(k)}$. A key observation here is that there is no explicit reference to the right-hand sides f or $\bar{f}$ in (13): the corresponding terms cancel both between the exact solution and the (exact) fine solver, and also between the two coarse solvers! Collecting the errors in the error vector $\boldsymbol{e}^{(k)} := \left(e_0^{(k)}, e_1^{(k)}, \ldots, e_N^{(k)}\right)^T$, we obtain from (13) the same fixed-point iteration as in [4]

$$\boldsymbol{e}^{(k+1)} = S\boldsymbol{e}^{(k)}, \tag{14}$$

where the matrix S is given by

$$S = \begin{bmatrix} 1 & & & 0 \\ -\mathcal{R}\left(\kappa\Delta T\right) & 1 & & \\ & \ddots & \ddots & \\ & & -\mathcal{R}\left(\kappa\Delta T\right) & 1 \end{bmatrix}^{-1} \begin{bmatrix} 0 & & & 1 \\ e^{-\kappa\Delta T} - \mathcal{R}\left(\kappa\Delta T\right) & 0 & & \\ & \ddots & \ddots & \\ & & e^{-\kappa\Delta T} - \mathcal{R}\left(\kappa\Delta T\right) & 0 \end{bmatrix}. \tag{15}$$

The asymptotic convergence factor of the fixed-point iteration (14) describing our new periodic Parareal algorithm (5)-(6) applied to the periodic problem (8) is therefore given by

$$\rho_{\text{asym}}(S) = \lim_{k\to\infty} \left(\|\boldsymbol{e}^{(k)}\| / \|\boldsymbol{e}^{(0)}\|\right)^{1/k}. \tag{16}$$

Theorem (Convergence estimate of the new periodic Parareal algorithm) Let $[0, T]$ be partitioned into N equal time intervals with $\Delta T = T/N$. Assume the fine propagator to be exact as in (9), and the coarse propagator to be a one-step method as in (11) satisfying (12). Then the asymptotic convergence factor (16) of the new periodic Parareal algorithm (5)-(6) is bounded for all $l \geq 1$ by

$$\rho_{\text{asym}}(S) < x_l, \text{ with } x_l = \left(\left|\mathcal{R}\left(\kappa\Delta T\right)\right| x_{l-1} + \left|e^{-\kappa\Delta T} - \mathcal{R}\left(\kappa\Delta T\right)\right|\right)^{\frac{N}{N+1}} \text{ and } x_0 = 1. \tag{17}$$

Proof Since the errors of the new periodic Parareal algorithm satisfy the same relation (14) as in [4], the proof follows by the same arguments as in [4]. □

We note that under the assumption (12), the operator S is a contraction [4], which ensures convergence of the new periodic Parareal algorithm (5)-(6).

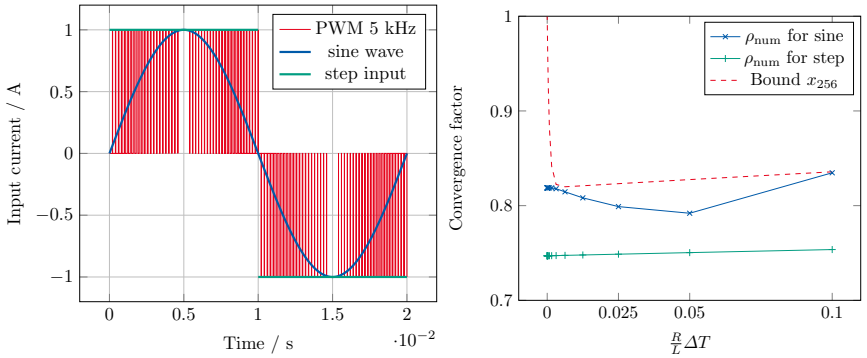

Fig. 1: Left: PWM excitation (19) of 5 kHz ($m = 100$) and two coarse inputs (20), (21). Right: convergence factor of the new periodic Parareal algorithm (5)-(6) with reduced coarse dynamics: sinusoidal waveform (20) and step function (21), together with our theoretical bound.

4 Numerical experiments for a model problem

In this section we illustrate our convergence theory for the new periodic Parareal algorithm with a periodic problem given by an RL-circuit model, namely

$$R^{-1}\phi'(t) + L^{-1}\phi(t) = f_m(t), \quad t \in (0,T), \qquad \phi(0) = \phi(T), \tag{18}$$

with the resistance $R = 0.01\ \Omega$, inductance $L = 0.001$ H, period $T = 0.02$ s, and f_m denoting the supplied PWM current source (in A) of 20 kHz, defined by

$$f_m(t) = \begin{cases} \operatorname{sign}\left[\sin\left(\frac{2\pi}{T}t\right)\right], & s_m(t) - \left|\sin\left(\frac{2\pi}{T}t\right)\right| < 0, \\ 0, & \text{otherwise}, \end{cases} \tag{19}$$

where $s_m(t) = \frac{m}{T}t - \left\lfloor \frac{m}{T}t \right\rfloor$, $t \in [0,T]$ is the common sawtooth pattern with $m = 400$ teeth. An example of the PWM signal of 5 kHz is shown in Fig. 1 on the left. This figure also illustrates the following two choices for the coarse excitation:

$$\bar{f}_{\text{sine}}(t) = \sin\left(\frac{2\pi}{T}t\right), \quad t \in [0,T] \tag{20}$$

$$\bar{f}_{\text{step}}(t) = \begin{cases} 1, & t \in [0, T/2], \\ -1, & t \in (T/2, T]. \end{cases} \tag{21}$$

We note that the step function (21) is discontinuous only at $t = T/2$. This does not lead to any difficulties, since we use Backward Euler for the time discretization and we choose the discontinuity to be located exactly at a synchronization point.

The coarse propagator $\bar{\mathcal{G}}$ then solves an IVP for the equation $R^{-1}\phi'(t) + L^{-1}\phi(t) = \bar{f}(t)$, $t \in (0,T]$, where the RHS $\bar{f}$ is one of the functions in (20) or (21). We

illustrate the estimate (17) by calculating the numerical convergence factor $\rho_{\text{num}} := \left(\|\boldsymbol{e}^{(K)}\|/\|\boldsymbol{e}^{(0)}\|\right)^{1/K}$ with the l^∞-norm of the error $\boldsymbol{e}^{(k)}$ at iteration $k \in \{0, K\}$ defined as

$$\|\boldsymbol{e}^{(k)}\| = \max_{0\le n\le N} |\phi(T_n) - \Phi_n^{(k)}|. \tag{22}$$

Here ϕ denotes the time-periodic steady-state solution of (18) having the same accuracy as the fine propagator, and $\Phi_n^{(K)}$ is the solution obtained at the Kth iteration when (5)-(6) converged up to a prescribed tolerance. The stability function used for x_l in (17) in case of Backward Euler is $\mathcal{R}\left(\frac{R}{L}\Delta T\right) = \left(1 + \frac{R}{L}\Delta T\right)^{-1}$.

On the right in Fig. 1, we show the measured convergence factor of the new Parareal iteration (5)-(6) for the two choices of the coarse excitation (20) and (21). The fine step size is chosen to be $\delta T = T/2^{18} \sim 7.63^{-8}$, while the coarse step varies as $\Delta T = T/2^p$, $p = 1, 2, \ldots, 17$. We also show on the right in Fig. 1 the value of x_{256} to be the bound in (17). The graphs show that the theoretical estimate is indeed an upper bound for the numerical convergence factor for both coarse inputs (sine and step). However, one can observe that x_{256} gives a sharper estimate in the case of the sinusoidal RHS (20), compared to the one defined in (21). We also noticed that the number of iterations required till convergence of (5)-(6) was the same (9 iterations on average for the values of ΔT considered) for both choices of the coarse input, while the initial error $\|\boldsymbol{e}^{(0)}\|$ was bigger with the step coarse input (21) than with the sinusoidal waveform (20). This led to a slightly smaller convergence factor in case of the step coarse input due to the definition of ρ_{num}.

5 Numerical experiments for an induction machine

We now test the performance of our new periodic Parareal algorithm with reduced coarse dynamics for the simulation of a four-pole squirrel-cage induction motor, excited by a three-phase PWM voltage source switching at 20 kHz. The model of this induction machine was introduced in [8]. We consider the no-load condition, when the motor operates with synchronous speed.

The spatial discretization of the two-dimensional cross-section of the machine with $n = 4400$ degrees of freedom leads to a time-periodic problem represented by the system of differential-algebraic equations (DAEs)

$$\mathbf{M}\mathrm{d}_t\mathbf{u}(t) + \mathbf{K}\left(\mathbf{u}(t)\right)\mathbf{u}(t) = \mathbf{f}(t), \quad t \in (0, T), \tag{23}$$

$$\mathbf{u}(0) = \mathbf{u}(T), \tag{24}$$

with unknown $\mathbf{u} : [0, T] \to \mathbb{R}^n$, (singular) mass matrix $\mathbf{M} \in \mathbb{R}^{n\times n}$, nonlinear stiffness matrix $\mathbf{K}(\cdot) : \mathbb{R}^n \to \mathbb{R}^{n\times n}$, and the T-periodic RHS $\mathbf{f} : [0, T] \to \mathbb{R}^n$, $T = 0.02$ s. The three-phase PWM excitation of period T in the stator under the no-load operation causes the T-periodic dynamics in $\mathbf{u}$ which allows the imposition of the periodic constraint (24). For more details regarding the mathematical model we refer to [5]. We would like to note that equation (23) is a DAE of index-1,

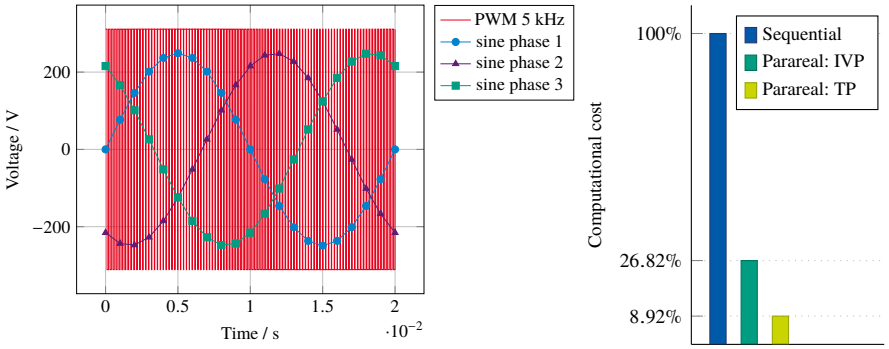

Fig. 2: Left: PWM excitation (19) of 5 kHz and three-phase sinusoidal voltage source of 50 Hz, used as the coarse input in our new periodic Parareal algorithm (5)-(6). Right: comparison of the computational costs calculated in terms of the effective number of linear algebraic systems solved for different approaches to obtain the periodic steady-state solution of the induction machine model.

which in case of discretization with Backward Euler can be treated essentially like an ODE [12].

We now use our new periodic Parareal algorithm (5)-(6) to find the solution of (23)-(24). The fine propagator $\mathcal{F}$ is then applied to (23) with the original three-phase PWM excitation of 20 kHz, discretized with the time step $\delta T = 10^{-6}$ s. The coarse solver $\bar{\mathcal{G}}$ uses a three-phase sinusoidal voltage source with frequency 50 Hz of the form (20), discretized with the time step $\Delta T = 10^{-3}$ s. Phase 1 of the PWM signal switching at 5 kHz as well as the applied periodic coarse excitation on $[0, 0.02]$ s are shown on the left in Fig. 2.

Both coarse and fine propagators solve the IVPs for (23) using Backward Euler, implemented within the GetDP library [7]. We used $N = 20$ time subintervals for the simulation of the induction machine with our new periodic Parareal algorithm, which converged after 14 iterations. Within these calculations 194 038 solutions of linearized systems of equations were performed effectively, i.e, when considering the fine solution cost only on one subinterval (due to parallelization) together with the sequential coarse solves.

On the other hand, a classical way to obtain the periodic steady-state solution is to apply a time integrator sequentially, starting from a zero initial value at $t = 0$. This computation reached the steady state after 9 periods, thereby requiring 2 176 179 linear system solves. Alternatively, one could apply the Parareal algorithm with reduced coarse dynamics, introduced in [5], to the IVP for (23) on $[0, 9T]$. In this case the simulation needed effectively 583 707 sequential linear solutions due to parallelization. However, in practice one would not know the number of periods beforehand and one could not optimally distribute the time intervals. We visualize this data on the right in Fig. 2. These results show that our new periodic Parareal algorithm (5)-(6) with reduced coarse dynamics (Parareal: TP) directly delivers the periodic steady-state solution about 11 times faster than the standard time integration (Sequential), and 3 times faster than the application of Parareal with the reduced dynamics (Parareal: IVP) to an IVP on $[0, 9T]$.

6 Conclusions

We introduced a new periodic Parareal algorithm with reduced dynamics, which is able to efficiently handle quickly-switching discontinuous excitations in time-periodic problems. We investigated its convergence properties theoretically, and illustrated them via application to a linear RL-circuit example. We then tested the performance of our new periodic Parareal algorithm in the simulation of a two-dimensional model of a four-pole squirrel-cage induction machine, and a significant acceleration of convergence to the steady state was observed. In particular, with our new periodic Parareal algorithm with reduced dynamics it is possible to obtain the periodic solution 11 times faster than when performing the classical time stepping.

References

1. Bermúdez, A., Domínguez, O., Gómez, D., Salgado, P.: Finite element approximation of nonlinear transient magnetic problems involving periodic potential drop excitations. Comput. Math. Appl. **65**(8), 1200–1219 (2013). DOI:10.1016/j.camwa.2013.02.019
2. Bose, B.K.: Power Electronics And Motor Drives. Academic Press, Burlington (2006)
3. Gander, M.J., Hairer, E.: Nonlinear convergence analysis for the parareal algorithm. In: Domain decomposition methods in science and engineering XVII, *Lect. Notes Comput. Sci. Eng.*, vol. 60, pp. 45–56. Springer, Berlin (2008). DOI:10.1007/978-3-540-75199-1_4
4. Gander, M.J., Jiang, Y.L., Song, B., Zhang, H.: Analysis of two parareal algorithms for time-periodic problems. SIAM J. Sci. Comput. **35**(5), A2393–A2415 (2013)
5. Gander, M.J., Kulchytska-Ruchka, I., Niyonzima, I., Schöps, S.: A new parareal algorithm for problems with discontinuous sources. SIAM J. Sci. Comput. **41**(2), B375–B395 (2019)
6. Gander, M.J., Vandewalle, S.: Analysis of the parareal time-parallel time-integration method. SIAM J. Sci. Comput. **29**(2), 556–578 (2007). DOI:10.1137/05064607X
7. Geuzaine, C.: GetDP: a general finite-element solver for the de Rham complex. In: PAMM, vol. 7, pp. 1010603–1010604. Wiley (2007). DOI:10.1002/pamm.200700750
8. Gyselinck, J., Vandevelde, L., Melkebeek, J.: Multi-slice FE modeling of electrical machines with skewed slots-the skew discretization error. IEEE Trans. Magn. **37**(5), 3233–3237 (2001)
9. Katagiri, H., Kawase, Y., Yamaguchi, T., Tsuji, T., Shibayama, Y.: Improvement of convergence characteristics for steady-state analysis of motors with simplified singularity decomposition-explicit error correction method. IEEE Trans. Magn. **47**(5), 1458–1461 (2011)
10. Lions, J.L., Maday, Y., Turinici, G.: Résolution d'EDP par un schéma en temps "pararéel". C. R. Acad. Sci. Paris Sér. I Math. **332**(7), 661–668 (2001). DOI:10.1016/S0764-4442(00)01793-6
11. Niyomsatian, K., Vanassche, P., Sabariego, R.V., Gyselinck, J.: Systematic control design for half-bridge converters with LCL output filters through virtual circuit similarity transformations. In: 2017 IEEE Energy Conversion Congress and Exposition (ECCE), pp. 2895–2902 (2017)
12. Schöps, S., Niyonzima, I., Clemens, M.: Parallel-in-time simulation of eddy current problems using parareal. IEEE Trans. Magn. **54**(3), 1–4 (2018). DOI:10.1109/TMAG.2017.2763090